Stem Cell Research (2014) 13, 61–74

Available online at www.sciencedirect.com

ScienceDirect

www.elsevier.com/locate/scr

Pelota regulates the development of extraembryonic endoderm through activation of bone morphogenetic protein (BMP) signaling

Gunsmaa Nyamsuren [a,1], Aleksandra Kata [a,1], Xingbo Xu [a], Priyadharsini Raju [a], Ralf Dressel [b], Wolfgang Engel [a], D.V. Krishna Pantakani [a], Ibrahim M. Adham [a,*]

[a] Institute of Human Genetics, University of Göttingen, D-37073 Göttingen, Germany
[b] Department of Cellular and Molecular Immunology, University of Göttingen, D-37075 Göttingen, Germany

Received 8 October 2013; received in revised form 10 March 2014; accepted 16 April 2014
Available online 26 April 2014

Abstract *Pelota* (*Pelo*) is ubiquitously expressed, and its genetic deletion in mice leads to embryonic lethality at an early post-implantation stage. In the present study, we conditionally deleted *Pelo* and showed that PELO deficiency did not markedly affect the self-renewal of embryonic stem cells (ESCs) or their capacity to differentiate in teratoma assays. However, their differentiation into extraembryonic endoderm (ExEn) in embryoid bodies (EBs) was severely compromised. Conversely, forced expression of *Pelo* in ESCs resulted in spontaneous differentiation toward the ExEn lineage. Failure of *Pelo*-deficient ESCs to differentiate into ExEn was accompanied by the retained expression of pluripotency-related genes and alterations in expression of components of the bone morphogenetic protein (BMP) signaling pathway. Further experiments have also revealed that attenuated activity of BMP signaling is responsible for the impaired development of ExEn. The recovery of ExEn and down-regulation of pluripotent genes in BMP4-treated *Pelo*-null EBs indicate that the failure of mutant cells to down-regulate pluripotency-related genes in EBs is not a result of autonomous defect, but rather to failed signals from surrounding ExEn lineage that induce the differentiation program. In vivo studies showed the presence of ExEn in *Pelo*-null embryos at E6.5, yet embryonic lethality at E7.5, suggesting that PELO is not required for the induction of ExEn development, but rather for ExEn maintenance or for terminal differentiation toward functional visceral endoderm which provides the embryos with growth factors required for further development. Moreover, *Pelo*-null fibroblasts failed to reprogram toward induced pluripotent stem cells (iPSCs) due to inactivation of BMP signaling and impaired mesenchymal-to-epithelial transition. Thus, our results indicate that PELO plays an important role in the establishment of pluripotency and differentiation of ESCs into ExEn lineage through activation of BMP signaling.

* Corresponding author at: Institute of Human Genetics, Heinrich-Düker-Weg 12, D-37073 Göttingen, Germany. Fax: +49 551 399303.
E-mail address: iadham@gwdg.de (I.M. Adham).
[1] These authors contributed equally to this work.

http://dx.doi.org/10.1016/j.scr.2014.04.011
1873-5061/

Introduction

Two developmental processes take place during pre-implantation in the development of mammalian embryos. The outer cells of the morula differentiate into a trophoectoderm (TE) lineage, whereas the inside cells become the inner cell mass (ICM). Further development involves the specification of the ICM into primitive endoderm (PrE), located on the outside of the ICM, and into epiblast (EPI) that differentiates during later embryonic development into all three germ layers, including primordial germ cells (Cockburn and Rossant, 2010). Around the time of implantation, PrE gives rise to extraembryonic endoderm (ExEn), which contributes to visceral (VE) and parietal endoderm (PE) (Tam and Loebel, 2007; Plusa et al., 2008). VE and PE enclose and provide the developing embryo with nutritive support and molecular signals that are essential for cell fate decisions and axial pattern initiation (Bielinska et al., 1999; Yamamoto et al., 2004). Genetic ablation studies of genes involved in the development of PrE or its derivatives revealed an early embryonic lethality (Molkentin et al., 1997; Morrisey et al., 1998; Koutsourakis et al., 1999; Yang et al., 2002). Recent reports revealed that the differential expression of the pluripotency-related gene *Nanog* and GATA family members *Gata4* and *Gata6* in ICM cells is responsible for cell fate decisions regarding differentiation into EPI and PrE, respectively (Chazaud et al., 2006). These results confirm previous findings that showed the requirement of *Nanog* for the establishment of EPI and for the suppression of PrE differentiation (Mitsui et al., 2003), whereas *Gata4* and *Gata6* are crucial for the development of PrE and its derivatives (Molkentin et al., 1997; Morrisey et al., 1998; Koutsourakis et al., 1999; Cai et al., 2009).

Embryonic stem cells (ESCs), the in vitro counterpart of ICM cells, are pluripotent and have the potential to differentiate into all cell lineages of the early embryo; hence, they are regarded as a valuable tool to understand the molecular mechanisms governing early embryonic development (Niwa, 2010). The embryoid body (EB) that is formed during ESC differentiation in floating culture critically mimics the pre- and post-implantation developmental stages of the embryo (Doetschman et al., 1985). This system was successfully exploited to study and understand the ExEn loss phenotype seen in a *Gata6*-knockout mouse model (Capo-Chichi et al., 2005).

PELO is highly conserved in eukaryotes. In yeast, the PELO-ortholog Dom34 and its interacting protein Hbs1 are the core components of the newly described RNA surveillance mechanism called No-Go decay (NGD) (Doma and Parker, 2006). NGD recognizes mRNAs on which the ribosome is stalled at a stable stem-loop, rare codon, or pseudoknot, triggering the endonucleolytic cleavage of these mRNAs (Graille et al., 2008; Chen et al., 2010). Despite central function of the Dom34:Hbs1 complex in NGD, neither of these proteins is essential for yeast survival (Carr-Schmid et al., 2002). In contrast, the deletion of *Pelo* results in embryonic lethality beyond 6.5 *dpc* in mice. The in vitro culture of $Pelo^{-/-}$ blastocysts revealed a failure of ICM to expand and give rise to ESCs, suggesting that PELO might be involved in the regulation of the cell cycle or the self-renewal of a pluripotent ICM or ESCs (Adham et al., 2003). The role of PELO in the control of germ stem cell self-renewal has been described in the ovary of *Drosophila melanogaster* (Xi et al., 2005).

Here, we generated a conditional knockout mouse model to investigate the role of PELO in early embryonic development and ESC pluripotency. We report that PELO is dispensable for self-renewal of ESCs but is required for ESC differentiation into ExEn. At the molecular level, we show that the decreased activity of BMP signaling is responsible for the impaired differentiation of ExEn in *Pelo*-deficient EBs.

Material and methods

Generation of conditional *Pelo* knockout mice

The $Pelo^{F}$ targeting construct was generated in the pPNT4 vector. In the $Pelo^{F}$ targeting construct, two loxP sites were inserted into intron 1 and the 3′-flanking region of *Pelo* to allow *Cre*-mediated recombination and excision of exons 2 and 3 containing the coding sequences of *Pelo*. The 6.7- and 4.6-kb long 5′- and 3′-flanking homologous arms, respectively, were cloned into the targeting construct (Suppl. Fig. 1A). The targeting vector was linearized with *Not*I and used for transfection of RI ESCs. Neomycin-resistant ESC clones were checked for homologous recombination by southern blot-analysis. External probes (P1 and P2 in Suppl. Fig. 1A) were used for hybridization of southern blots containing *Eco*RI- and *Bsr*GI-digested DNA (Suppl. Figs. 1B, C). To confirm the absence of the additional insertion of targeting construct in homologous recombinant ESCs, blots containing *Ase*I-digested DNA were probed with neomycin fragment (Suppl. Fig. 1D). Cells from two correctly targeted ESC clones were microinjected into C57BL/6J blastocysts. Chimeric founders were mated with C57BL/6J mice to generate heterozygous $Pelo^{F/+}$ mice, which were intercrossed with conventional $Pelo^{+/-}$ mice to produce heterozygous $Pelo^{F/-}$ mice. The *Rosa26CreERT2* knock-in (Hameyer et al., 2007) and transgenic *EIIa-Cre* mice (Lakso et al., 1996) were bred with $Pelo^{F/-}$ mice to generate inducible and constitutive *Pelo*-KO mice, respectively. Genotyping of mice was carried out by PCR amplification (Suppl. Fig. 1E). Primer sequences are listed in Suppl. Table 1.

All animal experiments were reviewed and approved by the Institutional Animal Care and Use Committee of the University of Göttingen.

Cell culture and teratoma formation assay

ESCs were maintained on Mitomycin C-treated MEF feeder layers in LIF-supplemented medium as described previously (Wurst and Joyner, 1993). For differentiation of ESCs into EBs, a single-cell suspension of ESCs was incubated for 30 min on uncoated culture dishes to remove feeder cells. Afterwards, ESCs (1×10^5 cells/cm^2) were plated onto bacteriological dishes and grown in ESC medium without LIF. After 4 days of culture, EBs were fed with fresh medium every second day and harvested at the indicated time points. Alternatively, MEF-free ESCs were plated on Aggriwell plates (STEMCELL Technologies) at a density of 1×10^5 cells/well. To determine whether the retinoic acid (RA) induces the ExEn differentiation in *Pelo*-null EBs, ESCs were allowed to aggregate and grown with 1 μM RA for 5 days. For culture of wild-type EBs with conditioned medium derived from *Pelo*-deficient EB cultures, $Pelo^{\Delta/-}$

ESCs were seeded at 5×10^4 cells per 1 cm^2 in Knockout™ DMEM medium supplemented with 20% Knockout™ serum replacement (SR, Life Technology) on bacterial Petri dishes. After 5 days of EB cultures, supernatants were collected, filtered and used as a culture medium for EB formation of wild-type ESCs. After 6 days, wild-type EBs were collected and either fixed for immunohistological analysis or subjected for RNA isolation.

To determine the effect of BMP4 and Noggin on the development of ExEn, mutant *Pelo*$^{\Delta/-}$ and control *Pelo*$^{F/-}$ EBs were formed in serum replacement medium (SR) supplemented with either 20 ng/ml recombinant BMP4 (Life Technology) or 150 ng/ml recombinant Noggin (Life Technology), respectively.

To generate BMP responsive reporter cell line (Pelo$^{F/-}$ BRE-FFLuc), *Pelo*$^{F/-}$ ESCs were transfected with the reporter construct pBFIR containing BMP responsive element (BRE) driven Firefly luciferase gene (FFLuc) and SV40 promoter/enhancer driven Renilla luciferase (RRLuc) gene (Yadav et al., 2012). The ESC clone (*Pelo*$^{F/-}$ *BRE-FFLuc*) showing high FFLuc activity in response to 20 ng/ml recombinant BMP4 was selected and cultured in medium containing 1 μM 4-OHT to generate *Pelo*$^{\Delta/-}$ *BRE-FFLuc* cell line. The parental *Pelo*$^{F/-}$ *BRE-FFLuc* and the *Pelo*$^{\Delta/-}$ *BRE-FFLuc* ESCs were aggregated in SR medium for 5 days, and the resulting EBs were then treated for 12 h either with or without 20 ng/ml recombinant BMP4. In another assay, *Pelo*$^{F/-}$ *BRE-FFLuc* EBs were cultured for 12 h with *Pelo*$^{\Delta/-}$ EBs conditioned medium supplemented either with or without BMP4. Dual luciferase assay was carried out according to the manufacturer's recommendation (PJK GmbH, Kleinblittersdorf, Germany).

For teratoma formation assay, single-cell suspension of cultured ESCs in PBS (4×10^6 cells in 100 μl PBS) was subcutaneously injected into the flanks of immunodeficient *RAG2*$^{-/-}$*gc*$^{-/-}$ mice. After 4–7 weeks, teratomas were excised, fixed, and subjected to histological analysis.

Generation of induced pluripotent stem cells

We used Yamanaka factors (retroviral expression vectors for *Oct3/4*, *Sox2*, *Klf4*, and *c-Myc*) procured from Addgene to generate iPSCs, as previously described (Takahashi and Yamanaka, 2006). Briefly, MEFs isolated from transgenic *Nanog*-EGFP (Okita et al., 2007), *Pelo*$^{F/+}$, *Pelo*$^{F/-}$, and *Pelo*$^{\Delta/-}$ MEFs were transduced with retroviral particles, as previously described (Xu et al., 2011). To establish iPSC lines, colonies that appeared after 10 days of virus infection were picked manually and cultured in 24-well plates under standard ESC culture conditions. For rescue experiments, *Pelo*$^{\Delta/-}$ MEFs were transduced with retroviral particles expressing *Pelo* in addition to Yamanaka factors.

Generation of expression constructs

The pCAG-Pelo-IZ construct used for the overexpression of *Pelo* in wild-type ESCs was generated by PCR amplification of *Pelo* cDNA using primers Pelo-F and Pelo-R (Suppl. Table 3) and cloning into the *Xho*I site of the pCAG-IZ vector. The construct containing the stem loop-EGFP (pCAG-SL-EGFP-IZ) was generated by PCR amplification and cloning of EGFP cassette (lacking ATG-start codon) into *Eco*RI/*Sal*I-digested pBluescript vector to yield pBluescript-EGFP. Sequences of primers (GFP-F and GFP-R) used for EGFP cassette amplification are provided in Supplementary Table S1. Next, the sense and anti-sense oligonucleotides SL-S and SL-AS (Suppl. Table 1) containing the sequences of ATG and stem-loop were annealed and cloned into the *Bam*HI/*Eco*RI-digested pBluescript-EGFP construct to generate pBluescript-SL-EGFP. Finally, the *Xho*I/*Sal*I fragment containing SL-EGFP fragment was cloned into *Xho*I-digested pCAGIZ vector to generate pCAG-SL-EGFP-IZ. The retroviral construct of *Pelo* (pMXs-Pelo) was generated by PCR amplification of *Pelo* cDNA using pcDNA 3.1-Myc-Pelo (Burnicka-Turek et al., 2010) as a template and cloning into *Eco*RI restriction sites of the pMX vector.

RNA isolation, RT-PCR, qRT-PCR, and northern blot analysis

Total RNA was extracted using an RNeasy mini-kit (Qiagen, Germany) or NucleoSpin miRNA kit (Macherey-Nagel, Germany) by following the manufacturer's protocols. For mRNA expression analysis, 5 μg total RNA was processed for cDNA synthesis using the SuperScript II system (Invitrogen, Germany). For miRNA quantification assays, 1 μg total RNA was used for cDNA synthesis using the miScript II RT Kit (Qiagen). For qRT-PCR analysis, diluted cDNA (1:10) was used as a template in a QuantiFast SYBR Green (Qiagen) reaction and run in an ABI 7900HT Real-Time PCR System (Applied Biosystems). Expression data were first normalized to housekeeping genes (*Hprt* or *Sdha*) and represented as relative expression to one of the cell types. For northern blot analysis, 15 μg total RNA was resolved on an agarose gel containing formaldehyde, transferred onto a nylon membrane, and hybridized with *Pelo* cDNA and EGFP probes (Shamsadin et al., 2002). All experiments were independently replicated at least two times. Primers used for RT-PCR and qRT-PCR analyses are listed in Supplementary Tables S2 and S3.

To assay *Noggin* mRNA stability in control and mutant cells, EBs were treated with 10 μg/ml of actinomycin D, and total RNA was extracted after 0, 0.5, 2, 4, and 8 h of the treatment. Northern blots with RNAs isolated from ESCs and EBs were hybridized with *Noggin* cDNA probe. Hybridization signals were quantified by ImageJ software (NIH, Bethesda, MD, USA). Optic density of *Noggin* mRNA levels at each time point was normalized to *Elongation factor-2* transcript levels.

Cell proliferation, apoptosis and cell cycle analysis

To determine cell proliferation, we used the CellTiter 96 AQueous Non-Radioactive Cell Proliferation Assay Kit (Promega, Madison, WI). Briefly, ESCs were plated at a density of 500 cells/well in gelatin-coated 96-well plates. After 2, 4, and 6 days of culture, cell proliferation was measured after incubation with MTS reagent. The absorbance was detected at 490 nm with a Microplate Reader. Results are presented as the mean absorbance of three independent experiments.

To verify the apoptosis, single-cell suspensions were labeled for Annexin-V and 7-amino-actinomycin D (7-AAD) staining using an Annexin V-PE Apoptosis Detection Kit I (BD

Biosciences), following the manufacturer's instructions. After staining, flow cytometric measurements were performed on a FACSCalibur flow cytometer and analyzed with CellQuestPro software (BD Biosciences).

For cell cycle analysis, ESCs were trypsinized and washed with PBS followed by ethanol fixation at 20 °C for a minimum of 2 h. After fixation, the cells were washed, resuspended in PBS containing 10 mg/ml propidium iodide (PI) and 1 mg/ml RNase A, and incubated at 37 °C for 30 min. After incubation, cells were measured on a FACSCalibur flow cytometer and analyzed after exclusion of cell doublets. All experiments were performed in three independent experiments.

Immunostaining and alkaline phosphatase staining

ESCs grown on cover slips were washed with phosphate-buffered saline (PBS) and fixed with 4% paraformaldehyde (PFA) at 4 °C for 30 min. EBs were fixed with 4% PFA at 4 °C for 1 h, washed with PBS, incubated with 30% sucrose at 4 °C, embedded in OCT, and cryosectioned at a 10-μm thickness. Deciduae were isolated at E6.5 and E7.5 from females of heterozygous *Pelo*$^{+/-}$ breeding, fixed overnight in 4% PFA at 4 °C, dehydrated and embedded in paraffin. Sections (5 μm) were either stained with hematoxylin and eosin (H&E) or subjected to immunohistological analysis. Cells or sections were permeabilized and blocked using PBS containing 0.1% Triton X-100 and 1% goat serum for 1 h. The primary antibodies were diluted in blocking buffer and incubated with cells or slides at 4 °C overnight. The next day, cells or slides were washed with PBS followed by incubation with secondary antibodies conjugated to fluorescent dyes. Images were acquired using an Olympus BX60 microscope (Olympus, Germany).

Cytochemical staining for alkaline phosphatase (AP) activity was performed using a Leukocyte Alkaline Phosphatase Kit (Sigma-Aldrich, Germany), according to the manufacturer's instructions.

Western blotting

Total protein isolation, separation by SDS-PAGE, and subsequent western blotting were performed as previously described (Xu et al., 2011). Antibodies used for western blot analysis and their sources are listed in Supplementary Table 4.

To determine the levels of Noggin in the conditioned medium, wild-type and *Pelo*-null EBs were cultured in SR medium. Conditioned medium was concentrated with Centrisart® I ultrafiltration unit (Sartorius, Germany). For semiquantitation of Noggin protein, equal amount of concentrates was loaded onto SDS/PAGE gel and blot was incubated with goat anti-mouse Noggin antibody (R&D systems).

TGF-β/BMP PCR array

A mouse TGFβ/BMP Signaling Pathway PCR array (SABiosciences, PAMM-035) was used to analyze the expression levels of BMP signaling pathway components in *Pelo*$^{F/-}$ and *Pelo*$^{\Delta/-}$ EBs. Briefly, total RNA was isolated from *Pelo*$^{F/-}$ and *Pelo*$^{\Delta/-}$ EBs after 5 days of ESC culture under differentiation conditions as described above. Subsequently, 5 μg total RNA was used for first-strand cDNA synthesis with the RT2 first strand kit (Qiagen, Germany). The PCR array was carried out following the manufacturer's instructions using the ready-to-use RT^2-qPCR master mix (RT2-SYBR® Green/Fluorescein qPCR master mix, SABiosciences, Germany). Twenty-five microliters of the experimental cocktail was added into each well containing pre-dispensed, gene-specific primer pairs and run on an ABI 7900HT fast quantitative PCR system. Data analysis was performed using the web-based standard RT PCR array suite (SABiosciences, Germany).

Statistical analysis

All qPCR data for RNA expression analysis (two or more biological replicates) were calculated using the standard curve method. A two-way ANOVA (GraphPad Prism 4.0) test was used to obtain calculations of statistical significance.

Results

PELO is essential for the development of ExEn lineage

To elucidate the function of *Pelo* in pluripotency and ESC differentiation potential, we generated a conditional *Pelo* construct containing two loxP elements flanking exons 2 and 3 of *Pelo* (Suppl. Fig. 1A). A floxed allele (*Pelo*^{F}) was generated in mouse ESCs by homologous recombination (Suppl. Figs. 1A–D). Injection of *Pelo*$^{F/+}$ ESCs into blastocysts resulted in chimeric mice, and further breeding with conventional heterozygous *Pelo*$^{+/-}$ established *Pelo*$^{F/-}$, whereas inbreeding with *Pelo*$^{F/+}$ established *Pelo*$^{F/F}$ animals. The *Pelo*$^{F/F}$ and *Pelo*$^{F/-}$ mice appeared normal and were fertile, indicating that the insertion of loxP and the neo-cassette did not disrupt the *Pelo* locus. Genetic depletion of *Pelo* in one cell-stage embryos was accomplished by breeding *Pelo*$^{F/F}$ with *Ella-Cre*-deleter mice and an F1 generation intercross of *Pelo* $^{\Delta/+}$*Ella-Cre* mice. Similar to the post-implantation lethality of conventional *Pelo*$^{-/-}$ embryos, genotyping of more than 100 embryos at E8.5 did not lead to the identification of any homozygous *Pelo*$^{\Delta/\Delta}$ embryos (data not shown), indicating that deletion of the floxed region in *Pelo*$^{\Delta/\Delta}$ embryos at the one-cell stage results in lethality.

To examine the consequence of *Pelo* deletion on ESC pluripotency and development of pre-implantation embryos, *Pelo*$^{F/-}$ mice were crossed with mice harboring a knock-in *Rosa 26-CreERT2* allele to obtain mice of the compound genotype *Pelo*$^{F/-}$*CreERT2* and *Pelo*$^{F/F}$ *CreERT2*.

We established *Pelo*$^{F/-}$*CreERT2* ESC lines that were derived from the ICM of blastocysts of *Pelo*$^{F/-}$*CreERT2* mice interbreeding. Upon 4-hydroxytamoxifen (4-OHT) treatment, *Cre*-mediated deletion of floxed *Pelo* generated a null allele (*Pelo*$^{\Delta}$), as verified by PCR (Suppl. Fig. 1E). Northern and western blot analyses confirmed the absence of the *Pelo* transcript and protein in *Pelo*$^{\Delta/-}$ ESCs (Suppl. Figs. 1F, G). *Pelo*-deficient ESCs exhibited normal colony morphology and unlimited proliferation in culture, but exhibiting slightly slower growth (Suppl. Fig. 2A). However, no alterations in the proportion of apoptotic cells were

observed when cells were analyzed based on Annexin-V and 7-aminoactinomycin D (7-AAD) staining by fluorescence-activated cell sorting (FACS) (Suppl. Fig. 2B). Furthermore, no significant differences were observed in the analyzed cell cycle parameters between control and *Pelo*-null ESCs (Suppl. Fig. 2C). The finding that the deletion of *Pelo* in established ESC lines did not significantly affect their viability was surprising, given that the conventional $Pelo^{-/-}$ ICM failed to expand its pluripotent cell population (Adham et al., 2003). Therefore, we studied the differentiation potential of mutant ESCs in formed embryoid bodies (EBs). In contrast with control $Pelo^{F/-}$ EBs, most of the mutant $Pelo^{\Delta/-}$ EBs failed to form a distinct outer layer of ExEn (Fig. 1A). We have determined the expression of several pluripotency and ExEn markers in control and mutant ESCs and EBs. No significant differences in expression levels of pluripotency genes were observed between mutant and control ESCs (Fig. 1C). The attenuated levels of *c-Myc* expression in mutant ESCs compared to that in control ESCs may explain the slightly slower growth of *Pelo*-deficient ESCs. Expression of pluripotency genes was markedly reduced in control $Pelo^{F/-}$ EBs, as expected (Fig. 1C). In contrast, pluripotency genes persist to express at high levels in *Pelo*-deficient EBs, even after 15 days of differentiation (Fig. 1C). Immunoblot analysis further confirmed the expression of OCT4 (also known as POU5F1) in *Pelo*-deficient EBs (Fig. 1B). Furthermore, re-plating of cells derived from 15-day-old $Pelo^{\Delta/-}$ EBs formed typical ESC colonies and expressed OCT4, whereas control $Pelo^{F/-}$ cells failed to form colonies (Suppl. Figs. 3A–D).

To confirm the impaired differentiation of ExEn in mutant $Pelo^{\Delta/-}$ EBs, we investigated the expression levels of marker genes for differentiation of ExEn lineage. As shown in Fig. 1D, expression levels of ExEn marker genes *Gata6*, *Gata4*, *Hnf4*, *Afp*, and *Dab2* were significantly reduced in mutant EBs. Immunostaining of histological sections of EBs revealed that expression of PELO and ExEn markers DAB2 and GATA4 is localized on the outer layer of control EBs, whereas PELO-, DAB2-, and GATA4-positive cells were mainly lacking in mutant EBs (Fig. 2A). Collectively, these results indicate a requirement of PELO for the development of ExEn lineage. We then investigated the consequence of *Pelo* deficiency on the temporal expression of genes associated with pluripotency, early and late stages of ExEn differentiation during EB formation (Fig. 2B). No significant differences in expression levels of pluripotency-related genes, *Nanog* and *Oct4*, in mutant and control EBs after 2 and 3 days of culture were observed. Similarly, there were no differences in the expression of early ExEn markers, *Gata4* and *Gata6*, after 3 days. After 4 days of EB formation, the expression of *Nanog* and *Oct4* was sharply down-regulated in control EBs compared to that in mutant EBs. In contrast, expression levels of *Gata4* and *Gata6* were significantly elevated in control EBs, but not in mutant EBs, after 5 days of culture (Fig. 2B). Unlike *Gata4* und *Gata6*, the expression of *Hnf4*, a late ExEn marker, was first activated in control EBs after 5 days of culture and subsequently enhanced. However, expression of *Hnf4* remained at low levels in *Pelo*-deficient EBs (Fig. 2B). The observed expression changes of early and late ExEn markers

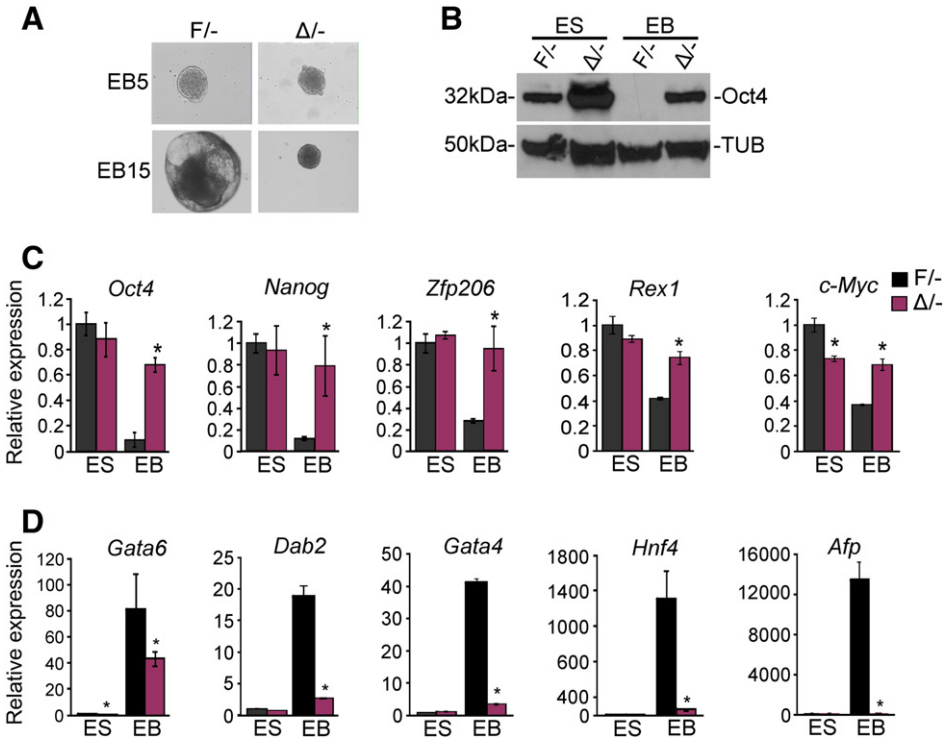

Figure 1 Failure of *Pelo*-deficient ESCs to differentiate into ExEn lineage. (A) Phase-contrast micrographs of control $Pelo^{F/-}$ and mutant $Pelo^{\Delta/-}$ EBs on days 5 (EB5) and 15 (EB15) of differentiation. (B) Immunoblot for expression of OCT4 in $Pelo^{F/-}$ and $Pelo^{\Delta/-}$ ESCs and EBs. (C) Quantitative real-time PCR analysis for the expression of pluripotency marker genes in $Pelo^{F/-}$ and $Pelo^{\Delta/-}$ ESCs and EBs on day 15 of differentiation. (D) Quantitative RT-PCR analysis of the expression of ExEn markers in $Pelo^{F/-}$ and $Pelo^{\Delta/-}$ ESCs and EBs. Values of expression levels in C and D normalized to *Hprt* or *Sdha* are presented as mean ± SD of three experiments. Transcript levels of control ESCs were expressed as 1.0. *, significantly different from control; $p < 0.05$.

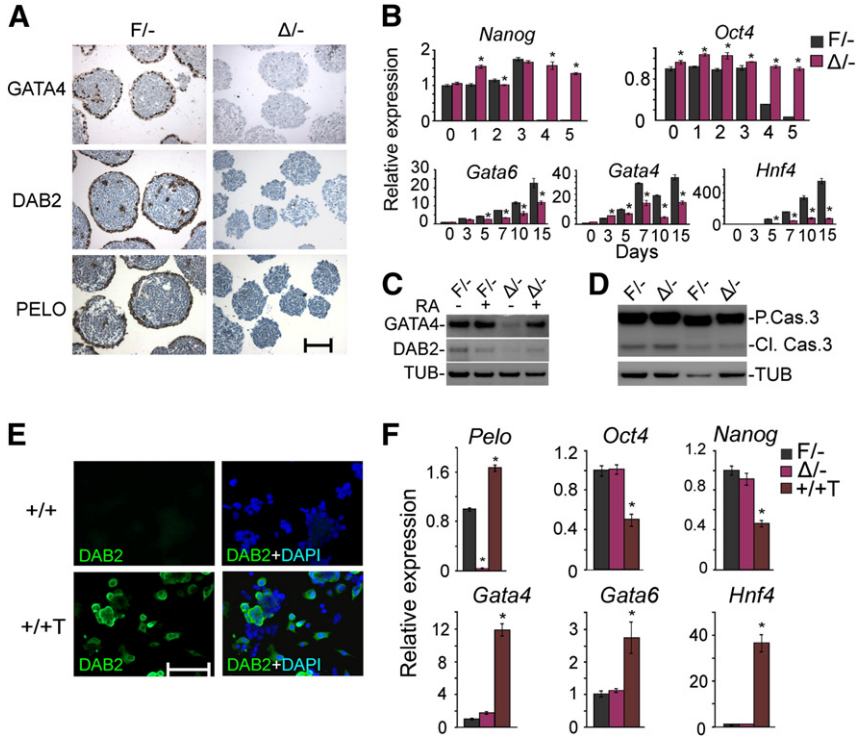

Figure 2 Expression of *Pelo* and ExEn markers in control $Pelo^{F/-}$ EBs, mutant $Pelo^{\Delta/-}$ EBs, and *Pelo*-overexpressing ESCs. (A) Paraffin sections of $Pelo^{F/-}$ and $Pelo^{\Delta/-}$ EBs on day 10 of differentiation were immunostained with GATA4, DAB2, and PELO antibodies. Scale bars in A: 20 μm. (B) Quantitative RT-PCR analysis for the temporal expression of pluripotency-related and ExEn markers in $Pelo^{F/-}$ and $Pelo^{\Delta/-}$ cells during EB formation. Expression levels normalized to *Hprt* are presented as mean ± SD of three experiments. Transcript levels of control cells at day 0 of differentiation were expressed as 1.0. *, significantly different from control; $p < 0.05$. (C) Immunoblot analysis for the expression of GATA4 and DAB2 in $Pelo^{F/-}$ and $Pelo^{\Delta/-}$ EBs, which were formed in the absence (−) or presence (+) of retinoic acid (RA). (D) Total proteins isolated from EBs after 10 days of culture were analyzed by immunoblotting for the expression of pro-caspase (P. cas.3) and cleaved caspase 3 (Cl. Cas.3). (E) Wild-type ESCs (+/+) and *Pelo*-overexpressing ESCs (+/+T) were cultured in the presence of LIF, fixed, and immunostained with anti-DAB2 antibodies. The nuclei were stained with DAPI. (F) Expression levels of *Pelo*, pluripotency and ExEn marker genes in $Pelo^{F/-}$, $Pelo^{\Delta/-}$ and *Pelo*-overexpressing ($Pelo^{+/+T}$) ESCs were determined by qRT-PCR. Values of expression levels normalized to *Hprt* are presented as mean ± SD of three experiments. Transcript levels of control ESCs were expressed as 1.0. *, significantly different from control; $p < 0.05$. Scale bars in E: 100 μm.

during EB formation suggest that the development of the ExEn is although induced in mutant EBs, but is not maintained to late stages of EB formation. We further investigated whether the impaired development of ExEn in *Pelo*-deficient EBs can be restored by the activation of retinoic acid (RT) signaling pathway. As shown in Fig. 2C, retinoic acid induces expression of GATA4 and DAB2 in *Pelo*-null EBs in the same extent as in control EBs, indicating that the RA treatment stimulates ExEn differentiation in *Pelo*-null EBs. To examine whether the impaired development of *Pelo*-null EBs is a result of increased apoptosis, we monitored apoptotic cell death by analyzing the levels of cleaved caspase 3 in control and mutant EBs after 10 days of culture. Western blot analysis revealed no marked difference in the protein levels of cleaved caspase 3 in both control and mutant EBs (Fig. 2D).

These results prompted us to examine whether overexpression of *Pelo* in wild-type ESCs induces a differentiation program toward ExEn. $Pelo^{+/+}$ ESCs were stably transfected with a pCAG-Pelo-IZ construct containing *Pelo* cDNA under the control of CAG promoter. In contrast to typical ESC morphology of empty vector-transfected cells, most *Pelo*-transfected colonies displayed closely apposed, flattened cells similar to the morphology of ExEn cells (Jetten et al., 1979) and were positive for DAB2 (Fig. 2E). Quantitative RT-PCR revealed that expression levels of *Pelo* in pCAG-Pelo-IZ-transfected cells were 1.7-fold higher than that of empty vector-transfected cells (Fig. 2F). In line with the DAB2 expression, the expression of *Gata4*, *Gata6* and *Hnf4* was strongly induced in *Pelo*-overexpressing cells (Fig. 2F). To determine whether increased expression of *Pelo* in ESCs restricts their fate to an ExEn lineage, expression of pluripotency genes *Oct4* and *Nanog* was examined. As shown in Fig. 2F, the expression of pluripotency marker genes was significantly reduced in *Pelo*-overexpressing cells, indicating that increased *Pelo* expression induces the differentiation of ESCs toward an ExEn lineage.

To assess the differentiation capacity of mutant ESCs in teratoma formation, we compared the teratoma-forming ability of control and mutant ESCs in immunodeficient $Rag2^{-/-}$ $cg^{-/-}$ mice. Both $Pelo^{F/-}$ and $Pelo^{\Delta/-}$ ESCs formed teratomas containing tissues derived from all three germ layers (Suppl. Fig. S4). These results revealed the capacity of *Pelo*-deficient ESCs to differentiate into cell lineages of the three germ layers in a teratoma assay.

Disrupted development of ExEn in EBs derived from mutant ESCs led us to investigate the development of ExEn in *Pelo*-null embryos. Since *Pelo*-deficient embryos died between E6.5 and E7.5 (Adham et al., 2003), we have performed immunohistological analysis on sections of E6.5 and E7.5 embryos derived from breeding of heterozygous $Pelo^{+/-}$ animals. As expected, PELO was ubiquitously expressed in control embryos, but was undetectable in $Pelo^{-/-}$ embryos (Suppl. Fig. 5A). Mutant E6.5 embryos were markedly smaller than their heterozygous and wild-type littermates. Although ExEn is formed in *Pelo*-deficient E6.5 embryos as indicated by the expression of GATA4 and DAB2, the development of *Pelo*-null embryos at E7.5 was severely affected, a likely consequence of the absence of ExEn (Suppl. Figs. 5A, B). These results suggest that PELO is not required for the formation of ExEn, but rather for the maintenance of ExEn or for terminal differentiation to functional ExEn that provides the embryo with growth factors required for early embryonic development.

PELO deficiency attenuates the activity of BMP signaling in EBs

Studies in *Drosophila* showed that PELO regulates the differentiation of germ stem cells in the ovary through BMP signaling (Xi et al., 2005). Interestingly, defects in a PrE-derived lineage, VE, and subsequent cavitation abnormalities were observed during EB formation of ESCs treated with BMP antagonists or ESCs overexpressing dominant-negative BMPR1b receptor (Coucouvanis and Martin, 1999; Conley et al., 2007; Rong et al., 2012). These observations, together with impaired ExEn development seen in *Pelo*-deficient EBs, led us to investigate the mRNA expression profile of genes involved in TGF-β/BMP signaling in control and mutant EBs. Gene expression analysis for TGF-β/BMP signaling components in a PCR array revealed that 22 genes exhibit at least a 3-fold difference in gene expression between *Pelo*-deficient and control EBs (Suppl. Fig. 6 and Table 5). The changes in mRNA levels of some differentially expressed genes were verified by qRT-PCR (Fig. 3A). The mRNA levels of several BMP ligand genes (*Bmp-4* and *-6*) were significantly down-regulated in *Pelo*-deficient EBs compared with control EBs (Fig. 3A). Additionally, the expression of several BMP-target genes, including *Id1* and *Id3*, was down-regulated in $Pelo^{\Delta/-}$ EBs, confirming the decreased activity of BMP signaling in mutant EBs (Fig. 3A). In contrast, genes encoding Noggin and Lefty1, which are known as potent antagonists of BMP and Nodal/Activin signaling, respectively, were expressed highly in mutant EBs to a level approximately more than 4–8 folds in control EBs (Fig. 3A). The decreased activity of BMP signaling in *Pelo*-deficient EBs was further confirmed by western blot analysis of phosphorylated Smad1/5 (Fig. 3B).

The strong up-regulation of *Noggin* in *Pelo*-deficient EBs was particularly interesting, because overexpression of *Noggin* has been shown to affect the ExEn development (Rong et al., 2012). Accordingly, we examined the effect of conditioned medium collected from *Pelo*-deficient EB culture on the differentiation of wild-type ESCs. While the expression of ExEn-specific markers was not significantly increased in *Pelo*-deficient EBs that were cultured in conditioned medium collected from wild-type EB culture (data not shown), culture of wild-type ESCs with conditioned medium collected from *Pelo*-deficient EB culture resulted in a significant decrease in expression levels of ExEn-specific markers (Fig. 3C). Moreover, we observed a decreased expression of BMP-targeted genes *Id1* and *Id3*, and a significant elevation of the pluripotency-related genes *Oct4* and *Nanog* (Fig. 3C). Western blotting with equal amount of concentrates of conditioned medium collected from wild-type and mutant EB cultures confirmed that Noggin was indeed expressed at higher levels in *Pelo*-null than in wild-type EB culture (Fig. 3D). These results indicate that increased levels of Noggin in conditioned medium derived from *Pelo*-deficient EB culture are responsible for the impaired ExEn development in wild-type EBs.

To confirm whether the decreased activity of BMP signaling in *Pelo*-deficient cells is responsible for the impaired ExEn development, mutant $Pelo^{\Delta/-}$ ESCs were aggregated and cultured in serum replacement medium (SR medium) supplemented with recombinant BMP4. Expression analysis showed that the expression of BMP-target genes *Id1* and *Id3*, and ExEn markers was significantly induced in BMP4-treated mutant EBs compared to that of BMP4-untreated EBs (Fig. 3E). The ExEn formation as judged by immunostaining further confirmed that the attenuated activity of BMP signaling is indeed responsible for impaired development of ExEn in *Pelo*-deficient EBs (Fig. 3F). A significant decrease in the expression levels of *Oct4* and *Nanog* was observed in mutant EBs grown in culture medium supplemented with BMP4 (Fig. 3E). These results suggest that the persistent expression of pluripotency genes in mutant EBs is not primarily due to PELO deficiency, but rather to failed development of ExEn in these EBs. Further experiments were performed to confirm previously reported results (Conley et al., 2007), which showed that the ExEn formation is disrupted in wild-type EBs grown in medium supplemented with Noggin (Figs. 3G, H).

To further verify the attenuated activity of BMP signaling in *Pelo*-null cells, we have established a BMP responsive reporter cell line ($Pelo^{F/-}$ *BRE-FFLuc*) by stably integrating BMP responsive dual luciferase reporter construct pBFIR (Yadav et al., 2012). The $Pelo^{F/-}$ *BRE-FFLuc* cell lines were treated with 4-OHT to generate mutant $Pelo^{\Delta/-}$ *BRE-FFLuc* ESCs. After growing EBs from both $Pelo^{F/-}$ *BRE-FFLuc* and $Pelo^{\Delta/-}$ *BRE-FFLuc* cell lines in SR medium, they were further cultured in medium supplemented either with or without BMP4. As shown in Fig. 3I, the relative FFLuc activities were increased significantly in BMP4-treated $Pelo^{F/-}$ *BRE-FFLuc* and $Pelo^{\Delta/-}$ *BRE-FFLuc* EBs. However, the relative FFLuc activity in control cells was significantly higher than that of mutant cells. In order to further examine the presence of BMP antagonists in the conditioned medium of $Pelo^{\Delta/-}$ EBs, relative FFLuc activities were measured in $Pelo^{F/-}$ *BRE-FFLuc* EBs that were treated for 12 h either with $Pelo^{\Delta/-}$ conditioned medium or with $Pelo^{\Delta/-}$ conditioned medium and BMP4. We observed that the relative FFLuc activity was significantly reduced in control $Pelo^{F/-}$ *BRE-FFLuc* EBs treated with $Pelo^{\Delta/-}$ conditioned medium compared to untreated control (Fig. 3M). This reduced activity was restored in control $Pelo^{F/-}$ *BRE-FFLuc* EBs, which were treated with both $Pelo^{\Delta/-}$ conditioned medium and BMP4 (Fig. 3M). Collectively, these results further confirm that the mutant $Pelo^{\Delta/-}$ EBs produce extracellular modulators of BMP signaling activity.

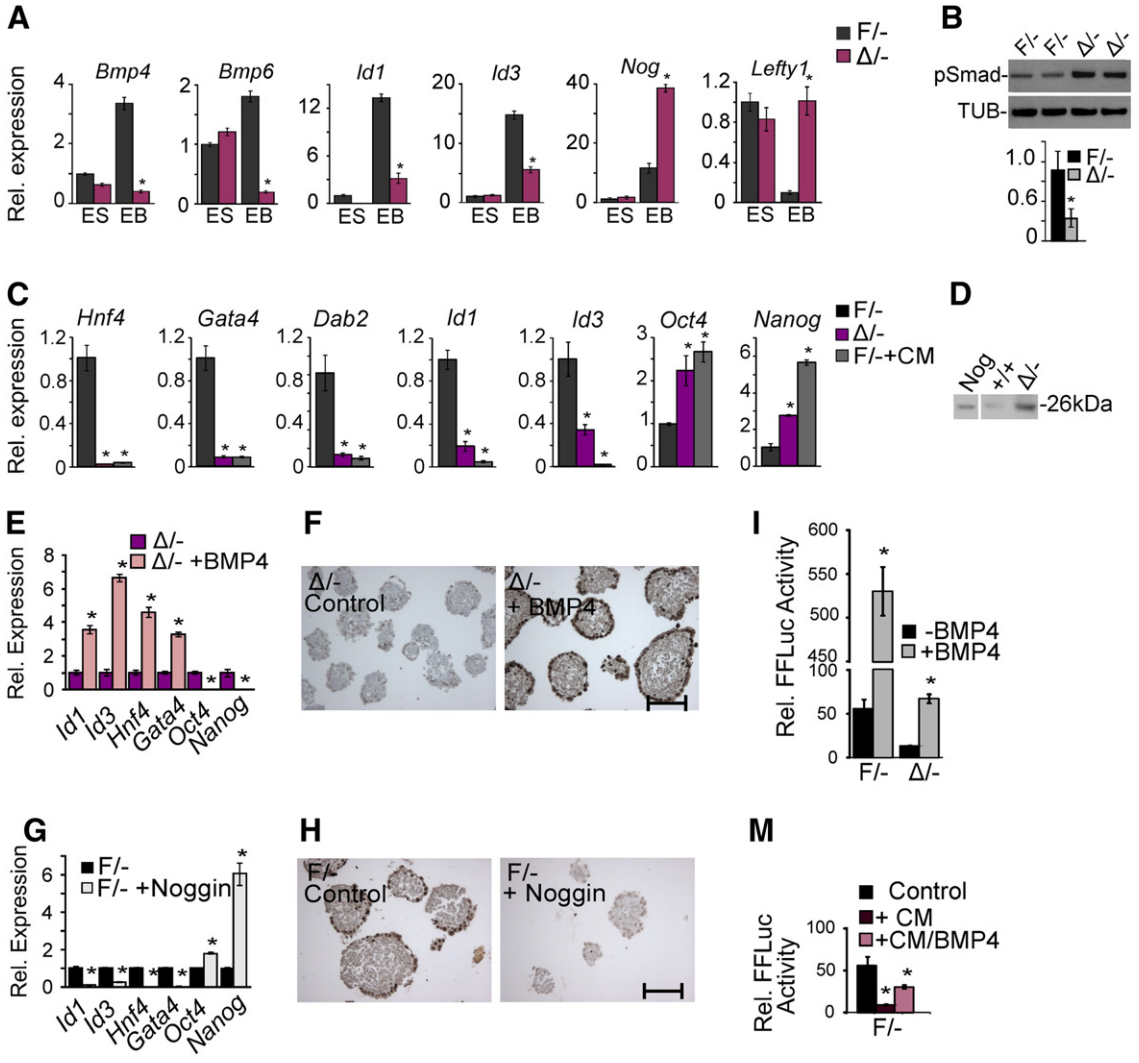

Figure 3 Attenuated activity of BMP signaling in $Pelo^{\Delta/-}$ EBs. (A) Quantitative RT-PCR analysis for expression of BMP ligands, BMP-target genes and antagonists (*Noggin* and *Lefty 1*) in control $Pelo^{F/-}$ and mutant $Pelo^{\Delta/-}$ ESCs and EBs on day 5 of differentiation. (B) Western blot analysis was performed to determine the expression levels of pSmad1/5 (pSmad) in control and mutant EBs (upper panel). In the bar graph presented in the lower panel, expression levels of pSmad1/5 were normalized to that of α-tubulin (TUB). Value is presented as mean ± SD. (C) Quantitative RT-PCR analysis for expression of ExEn, BMP-target genes and pluripotency markers in control $Pelo^{F/-}$, mutant $Pelo^{\Delta/-}$ EBs as well as control $Pelo^{F/-}$ EBs, which were cultured in conditioned medium derived from *Pelo*-deficient EB cultures ($Pelo^{F/-}$ + CM). Values of expression levels in A and C normalized to *Hprt* are presented as mean ± SD of three experiments. Transcript levels of control ESCs and EBs in A and C, respectively, were expressed as 1.0. *, significantly different from control ESCs (A) or EBs (C); $p < 0.05$. (D) Western blotting showing $Pelo^{\Delta/-}$-conditioned medium containing higher levels of Noggin than that in control-conditioned medium. Nog, 100 ng of recombinant Noggin was used as loading control. (E–H) Mutant $Pelo^{\Delta/-}$ and control $Pelo^{F/-}$ EBs, which were grown for 5 days in SR medium supplemented with either 20 ng/ml BMP4 (D, E) or 150 ng/ml Noggin (F, H), respectively, were subjected for RNA expression (E, G) and immunohistochemical analysis (F, H). (E, G) Quantitative RT-PCR analysis for expression of BMP-target, ExEn and pluripotency markers in BMP4-treated $Pelo^{\Delta/-}$ (E) and Noggin-treated $Pelo^{F/-}$ EBs (G). Values of expression levels in E and G normalized to *Hprt* are presented as mean ± SD of three experiments. Transcript levels of BMP4- and Noggin-untreated $Pelo^{\Delta/-}$ and $Pelo^{F/-}$ in E and G, respectively, were expressed as 1.0. *, significantly different from control BMP4-untreated $Pelo^{\Delta/-}$ EBs (E) and Noggin-untreated $Pelo^{F/-}$ EBs (G); $p < 0.05$. (F, H) Paraffin sections of mutant $Pelo^{\Delta/-}$ and control $Pelo^{F/-}$ EBs were immunostained with anti-GATA4 antibody. Paraffin sections and RNAs prepared from $Pelo^{\Delta/-}$ and $Pelo^{F/-}$ EBs, which grown only in SR medium, were used as untreated controls. Scale bars in F and H: 20 μm. (I) $Pelo^{F/-}$ FFLuc and $Pelo^{\Delta/-}$ FFLuc Luc ESCs were aggregated and grown in SR medium for 5 days and then treated for 12 h in SR medium supplemented either with or without BMP4. (M) $Pelo^{F/-}$ FFLuc EBs were cultured either with conditioned medium collected from mutant $Pelo^{\Delta/-}$ EBs or with conditioned medium collected from mutant $Pelo^{\Delta/-}$ EBs supplemented with BMP4. Relative FFLuc activity (FFLuc/RRLuc) in I and M is presented as mean ± SD of three experiments. *, significantly different from control cells; $p < 0.05$.

Pelo-depleted fibroblasts fail to generate iPSCs

To investigate whether *Pelo* is essential for the establishment of induced pluripotency in somatic cells, we performed reprogramming studies with mouse embryonic fibroblasts (MEFs) generated from controls (*Nanog*-EGFP, $Pelo^{F/+}$ and $Pelo^{F/-}$), and mutant $Pelo^{\Delta/-}$ embryos. Delivery of reprogramming factors, *Oct3/4*, *Sox2*, *Klf4*, and *c-Myc* (OSKM) into control, *Nanog-EGFP*, and $Pelo^{F/+}$ MEFs resulted in the appearance of AP-positive iPSC colonies (Figs. 4A, B), which were morphologically indistinguishable from ESC colonies and expressed pluripotency markers (data not shown). Delivery of reprogramming factors into *Pelo*-heterozygous $Pelo^{F/-}$ MEFs revealed a reduced number of AP-positive iPSC colonies (Figs. 4A, B). The established $Pelo^{F/-}$ iPSC colonies showed stereotypical colony morphology similar to ESCs and expressed pluripotency markers, such as SSEA1, Oct3/4, Sox2, and Nanog (Suppl. Figs. 7A, B). Interestingly, $Pelo^{\Delta/-}$ MEFs failed to reprogram and showed no AP-positive colonies (Figs. 4A, B). To verify whether overexpression of *Pelo* can rescue the inability of $Pelo^{\Delta/-}$ to yield iPSCs, we performed reprogramming studies by *Pelo* supplementation to the OSKM factors (Figs. 4C, D). Notably, the addition of *Pelo* greatly enhanced the iPSC generation from *Nanog*-EGFP, $Pelo^{F/+}$, and $Pelo^{F/-}$ MEFs, compared to OSKM alone (Figs. 4A–D). Moreover, we obtained iPSCs from $Pelo^{\Delta/-}$, confirming the rescue (Figs. 4C, D). To corroborate that *Pelo* deficiency does not lead to the loss of pluripotency once it is established, as observed for $Pelo^{\Delta/-}$ ESCs, we treated $Pelo^{F/-}$ iPSCs with 4-OHT. The homozygous deletion of *Pelo* in iPSCs ($Pelo^{\Delta/-}$) revealed smaller colony morphology and slower growth, as observed for $Pelo^{\Delta/-}$ ESCs, but were positive for AP-staining and pluripotency genes (Suppl. Fig. S7C and data not shown).

BMP and MET are misregulated during the reprogramming of *Pelo*-deficient fibroblasts

During the early phase of iPSC induction, an increase of BMP activity is necessary to promote mesenchymal-to-epithelial transition (MET) (Li et al., 2010; Samavarchi-Tehrani et al., 2010). Hence, we comparatively analyzed the expression of *Bmp6* and *Noggin* between days 6 and 9 of reprogramming of $Pelo^{F/+}$ and $Pelo^{\Delta/-}$ MEFs (Fig. 5A). The *Bmp6* expression was not upregulated in $Pelo^{\Delta/-}$ cells at day 6 of reprogramming, but was highly up-regulated in $Pelo^{F/+}$ MEFs (Fig. 5A). In agreement with these results, *Noggin* was dramatically down-regulated in control cells by day 6 of reprogramming (Fig. 5A). The slight change in expression levels of *Bmp6* and *Noggin* in $Pelo^{\Delta/-}$ cells persisted through day 9 of reprogramming (Fig. 5A). Simultaneously, we also analyzed the expression levels of both mesenchymal and epithelial

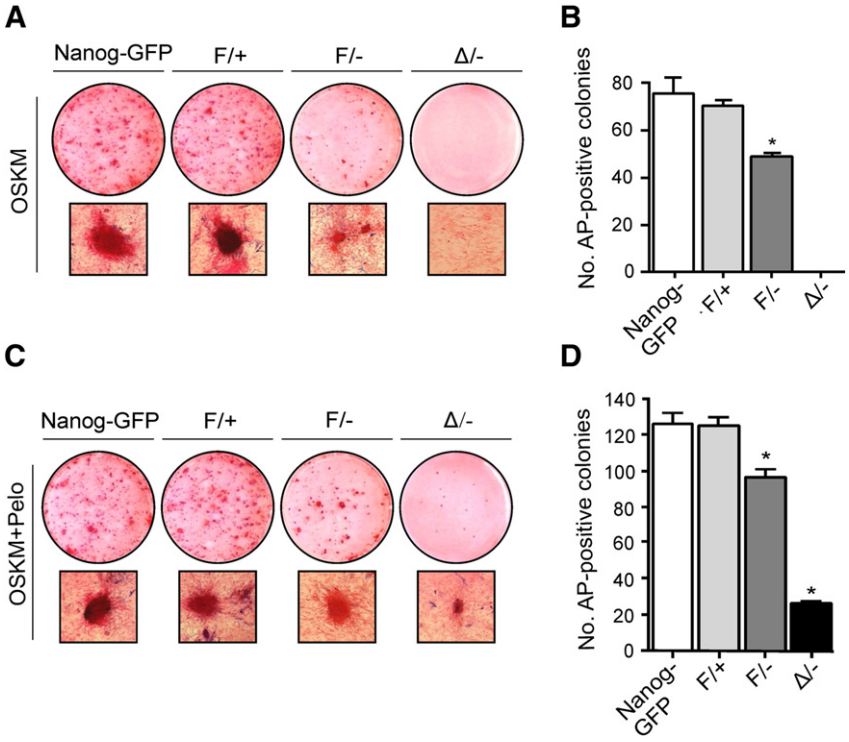

Figure 4 *Pelo* is required for somatic cell reprogramming. (A) Representative images of AP staining of various MEFs undergoing reprogramming with classical reprogramming factors (OSKM) (upper panel). High magnification of single colonies is shown in the lower panel. (B) The number of AP-positive colonies in reprogramming plates was counted 14 days post-transduction with OSKM vectors. Data are shown as the mean ± SD of three experiments. *, significantly different from control Nanog-GFP cells; $p < 0.05$. (C) Representative images of AP staining of various MEFs undergoing reprogramming with classical reprogramming factors (OSKM) together with *Pelo* (upper panel). High magnification of single colonies is shown in the lower panel. (D) The number of AP-positive colonies in reprogramming plates shown in D was counted 14 days post-transduction with OSKM together with *Pelo*. Data are shown as the mean ± SD of three experiments. *, significantly different from control Nanog-GFP cells; $p < 0.05$.

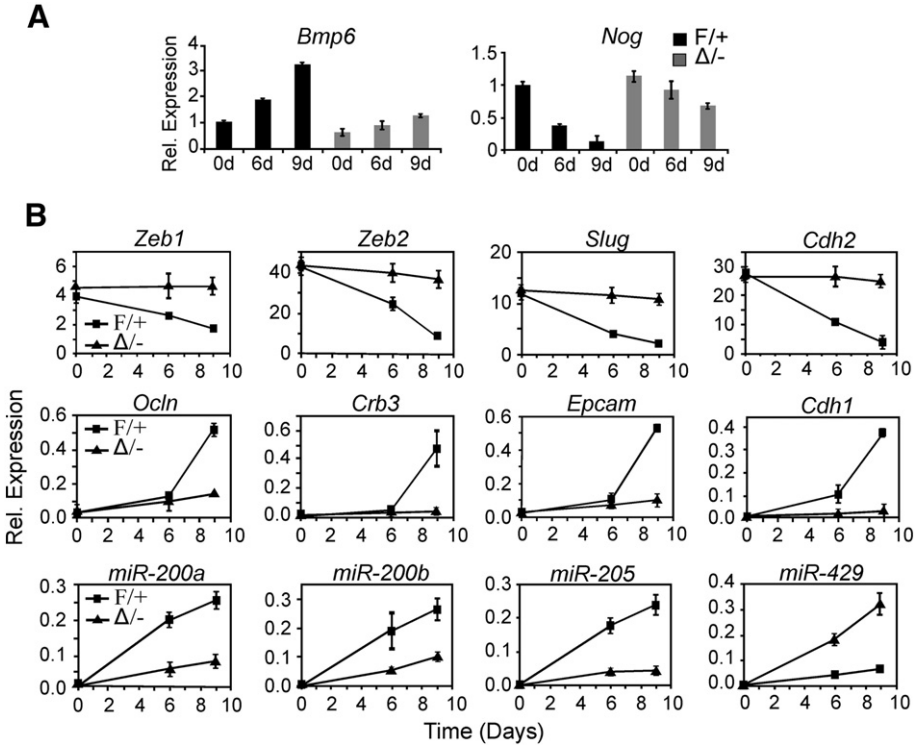

Figure 5 Expression of BMP signaling and MET components during the reprogramming of *Pelo*-deficient MEFs. (A) Expression of *Bmp6* and *Noggin* (*Nog*) in control $Pelo^{F/+}$ and mutant $Pelo^{\Delta/-}$ MEFs on days 0, 6 and 9 of reprogramming. Transcript levels in $Pelo^{F/-}$ MEFs on day 0 are shown as 1.0. (B) Line graphs showing the expression levels of mesenchymal and epithelial marker genes as well as miRNAs on days 0, 6, and 9 of reprogramming.

marker genes and miRNAs, which promote the MET, during the reprogramming of $Pelo^{\Delta/-}$ MEFs compared to control MEFs (Fig. 5B). The expression of mesenchymal marker genes (*Zeb1*, *Zeb2*, *Slug*, and *Cdh2*) was significantly down-regulated in $Pelo^{F/+}$, but their expression was unchanged or slightly reduced in $Pelo^{\Delta/-}$ MEFs even after 9 days of reprogramming (Fig. 5B). In line with these results, epithelial marker genes (*Ocln*, *Crb3*, *Epcam* and *Cdh1*) were highly up-regulated in reprogrammed control cells but not in $Pelo^{\Delta/-}$ cells (Fig. 5B). The expression of miRNAs (miR-200a, -200b, -205, and -429), which promote the MET process, was highly upregulated in $Pelo^{F/+}$ cells, but not in $Pelo^{\Delta/-}$ cells (Fig. 5B).

Conserved function of mammalian PELO in NGD

To determine whether the role of PELO in NGD is also conserved in mammalian cells, we analyzed control and Pelo-deficient ESCs for expression of the EGFP reporter gene (SL-EGFP) containing a stable stem loop (SL) located in frame with EGFP (Fig. 6A). Northern blot analysis revealed that EGFP-Zeo-fusion RNA was stable in mutant ESCs compared with control ESCs (Fig. 6B), whereas no EGFP-fluorescence and -protein were seen in either control or mutant ESCs (Fig. 6C and data not shown). These results suggest that ribosome stalled at stem-loop structure affects the translation of reporter mRNA in both mutant and wild-type ESCs and that the presence of PELO in wild-type ESCs might trigger the decay of EGFP mRNAs containing the stalled ribosomes. In contrast, the *Pelo*-deficient cells might be inefficient in activating the NGD, thereby accumulating the reporter mRNAs.

Significant increase in expression levels of *Noggin* in mutant EBs led us to examine the consequences of PELO depletion on the mRNA stability of *Noggin*. We performed actinomycin D chase experiments to monitor the post-transcriptional changes in levels of *Noggin* mRNA in $Pelo^{F/-}$ and $Pelo^{\Delta/-}$ cells. The mRNA levels of *Noggin* were gradually decreased after actinomycin D treatment with a similar time course in control and *Pelo*-null cells (Fig. 6D), indicating that the turnover of *Noggin* mRNA is not controlled by PELO-dependent mRNA decay.

Discussion

We previously reported that the conventional genetic depletion of *Pelo* in mouse results in an embryonic lethality at early post-implantation stages (Adham et al., 2003). Here, we report that *Pelo*-null ESCs are continuously propagated and retained their capacity to form undifferentiated colonies at clonal densities, but fail to differentiate into ExEn lineage in EBs. Conversely, overexpression of *Pelo* in ESCs led to down-regulation of pluripotency-related genes and a preferential activation of genes that regulate the differentiation of ESCs into an ExEn cell lineage.

Upon the aggregation of ES cells in suspension, the outer layer of developing EBs differentiates into ExEn, which deposits extracellular matrix into the underlying basement membrane (BM). Inside the BM, a primitive ectoderm layer is

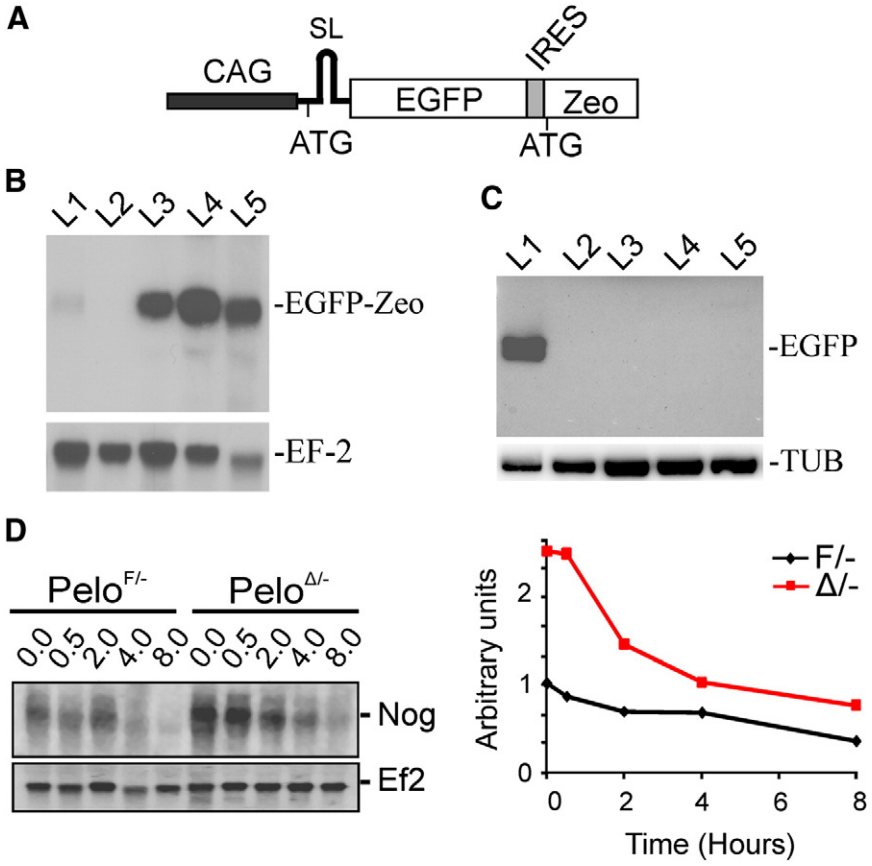

Figure 6 Conserved function of mammalian PELO in NGD. (A) Schematic diagram of the pCAG-SL-EGFP-ZEO construct. The stem loop (SL) sequence is located at the same reading frame with EGFP reporter gene. The internal ribosome entry site (IRES) is inserted between EGFP and zeocin (Zeo) resistant gene. (B) Blot containing RNA from SL-EGFP-overexpressing control *Pelo*$^{F/-}$ (L1), mutant *Pelo*$^{\Delta/-}$ ES clones (L3–L5) and untransfected ESCs (L2) was hybridized with an EGFP probe. (C) Blot with protein extracts from SL-EGFP-overexpressing *Pelo*$^{F/-}$ (L2, L3) and *Pelo*$^{\Delta/-}$ ES clones (L4, L5) and *Vsig-EGFP* transgenic stomach as a control (L1) was probed with anti-GFP antibody. The membrane was subsequently reprobed with α-tubulin antibody. (D) *Noggin* mRNA stability in control *Pelo*$^{F/-}$ and mutant *Pelo*$^{\Delta/-}$ EBs. Control and *Pelo*-deficient EBs were treated with actinomycin D, and total RNA was isolated after 0, 0.5, 2, 4 and 8 h of treatments. RNA blots were hybridized with *Noggin* cDNA probe. Expression levels of *Nanog* were normalized to corresponding *EF-2* mRNA levels. The normalized levels in control cells at time 0 were expressed as 1.00, and all other normalized mRNA levels were graphed relative to that value (left panel).

developed, and cavitation is formed in the core of the EBs (Niwa, 2010). The developmental process of EBs mimics the early embryonic stages of late blastocyst to egg cylinder (E4.5–E6.5). Both formation of ExEn and cavitation have been shown to be regulated by the BMP signaling pathway in mouse embryos and EBs. Thus, inhibition of BMP signaling by expression of a dominant-negative BMP receptor, down-regulation of *Bmp6* expression in ectodermal cells or addition of the BMP antagonist Noggin in culture prevents the development of ExEn in EBs (Coucouvanis and Martin, 1999; Conley et al., 2007; Rong et al., 2012). A significant decrease in the expression levels of BMP-targeted genes, phosphorylated Smad1/5, and the overexpression of *Noggin* in *Pelo*-deficient EBs suggest that PELO regulates differentiation toward ExEn lineage through the activation of BMP signaling. These results were supported by the observations of restored ExEn development in mutant EBs grown in medium supplemented with BMP4. Further, the negative effect of conditioned medium collected from mutant EBs on the ExEn formation in wild-type EBs and the significant decrease of luciferase activity in the BMP responsive reporter cell line indicate that mutant EBs secrete extracellular modulators which attenuate the BMP signaling activity.

Several factors regulate the activity of BMP signaling at intracellular and extracellular levels. The responsiveness of wild-type and mutant cells to Noggin and BMP4 treatment excludes the role of PELO in regulation of the intracellular modulators of BMP signaling. Extracellular modulators such as Noggin and Chordin antagonize the BMP signal (Piccolo et al., 1996; Zimmerman et al., 1996). Acute overexpression of *Noggin* in *Pelo*-null EBs led to suggest that PELO regulates the BMP signaling by negatively regulating *Noggin* expression at either transcriptional or post-transcriptional levels. Cytoplasmic localization of PELO in human and *Drosophila* cells (Xi et al., 2005; Burnicka-Turek et al., 2010) rules out that PELO directly regulates *Noggin* at the transcriptional level. In addition, the fact that the conserved role of PELO in NGD and deletion of PELO do not affect the stability of

Noggin transcripts suggests that PELO indirectly down-regulates *Noggin* through controlling stability of transcription factors regulating *Noggin* expression. Taken together, these results led us to conclude that the reduced BMP signaling in *Pelo*-null EBs accounts for the observed defect in ExEn differentiation. In support of our results, impaired ExEn development as a result of the affected BMP signaling was also shown in Smad4-deficient EBs (Sirard et al., 1998).

Moreover, BMP-mediated MET activation was shown to be essential for the induction of pluripotency in somatic cells (Li et al., 2010; Samavarchi-Tehrani et al., 2010). The failure of *Pelo*-deficient MEFs to activate BMP signaling during reprogramming reinforces that PELO is an indispensable component for the activation of BMP signaling during the establishment of pluripotency and ExEn cell lineage commitment.

The failure of *Pelo*-null ESCs to undergo ExEn differentiation was accompanied by a significant decrease in the expression levels of the transcription factors *Gata4*, *Gata6* and *Hnf4*, which are involved in differentiation and functions of ExEn lineage. Similarly, ESCs lacking either *Gata4* or *Gata6* failed to form the endodermal outer layer (Soudais et al., 1995; Morrisey et al., 1998). Like the overexpression of *Gata4* and *Gata6* (Fujikura et al., 2002), forced expression of *Pelo* directs differentiation of ExEn lineage in ESCs. Remarkably, the expression levels of the *Pelo* transcript were approximately 1.7-fold higher than that of wild-type ESCs. However, this modest change was sufficient to induce differentiation of ESCs into cells positive for ExEn markers, suggesting a quantitative effect of *Pelo* on ESC differentiation.

The recovery of ExEn outer layer and down-regulation of pluripotent genes in mutant EBs grown in medium supplemented with BMP4 indicate that the failure of *Pelo*-null cells to down-regulate pluripotency-related genes in EBs is not a result of cell-autonomous effect, but rather to failed signals from surrounding ExEn that induce the differentiation program. These findings are in agreement with the results showing that the persistence of pluripotent cells in *Dido 3*-deficient EBs is a result of the failed ExEn development (Futterer et al., 2012). The differentiation of *Pelo*-deficient ESCs to different germ layers in teratoma assay and to ExEn in response to retinoic acid confirms that the loss of PELO does not impair the differentiation of ESCs. Further in vivo studies showed the presence of ExEn in *Pelo*-null embryos at E6.5 and embryonic lethality at E7.5. These results led us to suggest that PELO is not required for the induction of ExEn, but rather for the maintenance or terminal differentiation toward functional visceral endoderm. Like *Pelo* mutants, targeted deletion of *Gata6*, *Dab2* and *Hnf4* genes, which are initially expressed in ExEn, resulted in early embryonic lethality. Despite the failed development of ExEn in the *Gata6*-, *Dab2*- and *Hnf4*-deficient EBs, ExEn is formed in their mutant E6.5 embryos (Duncan et al., 1997; Morrisey et al., 1998; Yang et al., 2002). These studies have attributed the affected development of mutant embryos to deficiency of functional ExEn. Restoration of ExEn development in *Pelo*-null EBs by supplementation of RA led us to suggest that RA-regulated pathway might have induced the ExEn differentiation in *Pelo*-null embryo at E6.5.

Our experiments showed that PELO deficiency inhibits the reprogramming of somatic cells, whereas the overexpression of *Pelo* along with other reprogramming factors promotes efficient reprogramming. These results suggest that PELO is required during the initiation stage of reprogramming, and its loss impairs the process. Recent reports revealed that increased BMP signaling during the initial stages of reprogramming promotes the MET (Li et al., 2010; Samavarchi-Tehrani et al., 2010). The failure of BMP signaling activation in $Pelo^{\Delta/-}$ cells undergoing reprogramming suggests a critical role of PELO in the early phase of somatic reprogramming, probably by activating BMP signaling. Consistent with the absence of reprogramming in $Pelo^{\Delta/-}$ cells, the expression levels of mesenchymal and epithelial markers in $Pelo^{\Delta/-}$ reprogrammed cells were not significantly altered compared to those in parental $Pelo^{\Delta/-}$ MEF cells.

Collectively, our results highlight the role of PELO in the activation of BMP signaling in order to drive the establishment of pluripotency and ExEn lineage. Further studies aimed at the identification and characterization of protein complexes containing PELO and how PELO activates BMP signaling will shed light on the function of PELO in these processes.

Acknowledgments

This work was supported in part by DFG grant Ad 129/2 to I.M.A. and by University Medical Center of Göttingen (Forschungsförderungsprogramm) to I.M.A. We are grateful to L.K. Dörfel (Institute of Human Genetic, Göttingen) for kindly helping us in characterization and analyses of *Pelo*-deficient ESCs and mice. We thank J. Nolte (Institute of Human Genetic, Göttingen) for her help in protein analysis; M. Schindler and U. Fünfschilling (MPI for Experimental Medicine, Göttingen) for their help in the generation of knockout mice; A. Nagy (Mount Sinai Hospital, Toronto) for providing RI ES cells; M. Conrad (Institute of Clinical Molecular Biology and Tumor Genetics, GSF, Munich) for providing pPNT4; A. Berns and A. Loonstra (The Netherlands Cancer Institute, Amsterdam) for providing Rosa 26 Cre ERT2 mice; and H. Niwa (Riken Center, Kobe, Japan) and A. Bandyopadhyay (Indian Institute of Technology, Kanpur, India) for providing CAG-IRES-ZEO and pBFIR vector, respectively.

Appendix A. Supplementary data

Supplementary data to this article can be found online at http://dx.doi.org/10.1016/j.scr.2014.04.011.

References

Adham, I.M., Sallam, M.A., Steding, G., Korabiowska, M., Brinck, U., Hoyer-Fender, S., Oh, C., Engel, W., 2003. Disruption of the pelota gene causes early embryonic lethality and defects in cell cycle progression. Mol. Cell. Biol. 23, 1470–1476.

Bielinska, M., Narita, N., Wilson, D.B., 1999. Distinct roles for visceral endoderm during embryonic mouse development. Int. J. Dev. Biol. 43, 183–205.

Burnicka-Turek, O., Kata, A., Buyandelger, B., Ebermann, L., Kramann, N., Burfeind, P., Hoyer-Fender, S., Engel, W., Adham, I.M., 2010. Pelota interacts with HAX1, EIF3G and SRPX and the resulting protein complexes are associated with the actin cytoskeleton. BMC Cell Biol. 11, 28.

Cai, K.Q., Caslini, C., Capo-chichi, C.D., Slater, C., Smith, E.R., Wu, H., Klein-Szanto, A.J., Godwin, A.K., Xu, X.X., 2009. Loss of GATA4

and GATA6 expression specifies ovarian cancer histological subtypes and precedes neoplastic transformation of ovarian surface epithelia. PLoS One 4, e6454.
Capo-Chichi, C.D., Rula, M.E., Smedberg, J.L., Vanderveer, L., Parmacek, M.S., Morrisey, E.E., Godwin, A.K., Xu, X.X., 2005. Perception of differentiation cues by GATA factors in primitive endoderm lineage determination of mouse embryonic stem cells. Dev. Biol. 286, 574–586.
Carr-Schmid, A., Pfund, C., Craig, E.A., Kinzy, T.G., 2002. Novel G-protein complex whose requirement is linked to the translational status of the cell. Mol. Cell. Biol. 22, 2564–2574.
Chazaud, C., Yamanaka, Y., Pawson, T., Rossant, J., 2006. Early lineage segregation between epiblast and primitive endoderm in mouse blastocysts through the Grb2–MAPK pathway. Dev. Cell 10, 615–624.
Chen, L., Muhlrad, D., Hauryliuk, V., Cheng, Z., Lim, M.K., Shyp, V., Parker, R., Song, H., 2010. Structure of the Dom34–Hbs1 complex and implications for no-go decay. Nat. Struct. Mol. Biol. 17, 1233–1240.
Cockburn, K., Rossant, J., 2010. Making the blastocyst: lessons from the mouse. J. Clin. Invest. 120, 995–1003.
Conley, B.J., Ellis, S., Gulluyan, L., Mollard, R., 2007. BMPs regulate differentiation of a putative visceral endoderm layer within human embryonic stem-cell-derived embryoid bodies. Biochem. Cell Biol. 85, 121–132.
Coucouvanis, E., Martin, G.R., 1999. BMP signaling plays a role in visceral endoderm differentiation and cavitation in the early mouse embryo. Development 126, 535–546.
Doetschman, T.C., Eistetter, H., Katz, M., Schmidt, W., Kemler, R., 1985. The in vitro development of blastocyst-derived embryonic stem cell lines: formation of visceral yolk sac, blood islands and myocardium. J. Embryol. Exp. Morphol. 87, 27–45.
Doma, M.K., Parker, R., 2006. Endonucleolytic cleavage of eukaryotic mRNAs with stalls in translation elongation. Nature 440, 561–564.
Duncan, S.A., Nagy, A., Chan, W., 1997. Murine gastrulation requires HNF-4 regulated gene expression in the visceral endoderm: tetraploid rescue of Hnf-4(−/−) embryos. Development 124, 279–287.
Fujikura, J., Yamato, E., Yonemura, S., Hosoda, K., Masui, S., Nakao, K., Miyazaki Ji, J., Niwa, H., 2002. Differentiation of embryonic stem cells is induced by GATA factors. Genes Dev. 16, 784–789.
Futterer, A., Raya, A., Llorente, M., Izpisua-Belmonte, J.C., de la Pompa, J.L., Klatt, P., Martinez, A.C., 2012. Ablation of Dido3 compromises lineage commitment of stem cells in vitro and during early embryonic development. Cell Death Differ. 19, 132–143.
Graille, M., Chaillet, M., van Tilbeurgh, H., 2008. Structure of yeast Dom34: a protein related to translation termination factor Erf1 and involved in No-Go decay. J. Biol. Chem. 283, 7145–7154.
Hameyer, D., Loonstra, A., Eshkind, L., Schmitt, S., Antunes, C., Groen, A., Bindels, E., Jonkers, J., Krimpenfort, P., Meuwissen, R., et al., 2007. Toxicity of ligand-dependent Cre recombinases and generation of a conditional Cre deleter mouse allowing mosaic recombination in peripheral tissues. Physiol. Genomics 31, 32–41.
Jetten, A.M., Jetten, M.E., Sherman, M.I., 1979. Stimulation of differentiation of several murine embryonal carcinoma cell lines by retinoic acid. Exp. Cell Res. 124, 381–391.
Koutsourakis, M., Langeveld, A., Patient, R., Beddington, R., Grosveld, F., 1999. The transcription factor GATA6 is essential for early extraembryonic development. Development 126, 723–732.
Lakso, M., Pichel, J.G., Gorman, J.R., Sauer, B., Okamoto, Y., Lee, E., Alt, F.W., Westphal, H., 1996. Efficient in vivo manipulation of mouse genomic sequences at the zygote stage. Proc. Natl. Acad. Sci. U. S. A. 93, 5860–5865.
Li, R., Liang, J., Ni, S., Zhou, T., Qing, X., Li, H., He, W., Chen, J., Li, F., Zhuang, Q., et al., 2010. A mesenchymal-to-epithelial transition initiates and is required for the nuclear reprogramming of mouse fibroblasts. Cell Stem Cell 7, 51–63.
Mitsui, K., Tokuzawa, Y., Itoh, H., Segawa, K., Murakami, M., Takahashi, K., Maruyama, M., Maeda, M., Yamanaka, S., 2003. The homeoprotein Nanog is required for maintenance of pluripotency in mouse epiblast and ES cells. Cell 113, 631–642.
Molkentin, J.D., Lin, Q., Duncan, S.A., Olson, E.N., 1997. Requirement of the transcription factor GATA4 for heart tube formation and ventral morphogenesis. Genes Dev. 11, 1061–1072.
Morrisey, E.E., Tang, Z., Sigrist, K., Lu, M.M., Jiang, F., Ip, H.S., Parmacek, M.S., 1998. GATA6 regulates HNF4 and is required for differentiation of visceral endoderm in the mouse embryo. Genes Dev. 12, 3579–3590.
Niwa, H., 2010. Mouse ES cell culture system as a model of development. Dev. Growth Differ. 52, 275–283.
Okita, K., Ichisaka, T., Yamanaka, S., 2007. Generation of germline-competent induced pluripotent stem cells. Nature 448, 313–317.
Piccolo, S., Sasai, Y., Lu, B., De Robertis, E.M., 1996. Dorsoventral patterning in *Xenopus*: inhibition of ventral signals by direct binding of chordin to BMP-4. Cell 86, 589–598.
Plusa, B., Piliszek, A., Frankenberg, S., Artus, J., Hadjantonakis, A.K., 2008. Distinct sequential cell behaviours direct primitive endoderm formation in the mouse blastocyst. Development 135, 3081–3091.
Rong, L., Liu, J., Qi, Y., Graham, A.M., Parmacek, M.S., Li, S., 2012. GATA-6 promotes cell survival by up-regulating BMP-2 expression during embryonic stem cell differentiation. Mol. Biol. Cell 23, 3754–3763.
Samavarchi-Tehrani, P., Golipour, A., David, L., Sung, H.K., Beyer, T.A., Datti, A., Woltjen, K., Nagy, A., Wrana, J.L., 2010. Functional genomics reveals a BMP-driven mesenchymal-to-epithelial transition in the initiation of somatic cell reprogramming. Cell Stem Cell 7, 64–77.
Shamsadin, R., Adham, I.M., Engel, W., 2002. Mouse pelota gene (Pelo): cDNA cloning, genomic structure, and chromosomal localization. Cytogenet. Genome Res. 97, 95–99.
Sirard, C., de la Pompa, J.L., Elia, A., Itie, A., Mirtsos, C., Cheung, A., Hahn, S., Wakeham, A., Schwartz, L., Kern, S.E., et al., 1998. The tumor suppressor gene Smad4/Dpc4 is required for gastrulation and later for anterior development of the mouse embryo. Genes Dev. 12, 107–119.
Soudais, C., Bielinska, M., Heikinheimo, M., MacArthur, C.A., Narita, N., Saffitz, J.E., Simon, M.C., Leiden, J.M., Wilson, D.B., 1995. Targeted mutagenesis of the transcription factor GATA-4 gene in mouse embryonic stem cells disrupts visceral endoderm differentiation in vitro. Development 121, 3877–3888.
Takahashi, K., Yamanaka, S., 2006. Induction of pluripotent stem cells from mouse embryonic and adult fibroblast cultures by defined factors. Cell 126, 663–676.
Tam, P.P., Loebel, D.A., 2007. Gene function in mouse embryogenesis: get set for gastrulation. Nat. Rev. Genet. 8, 368–381.
Wurst, W., Joyner, A.L., 1993. Production of targeted embryonic stem cell clones, In: Joyner, A.L. (Ed.), Gene Targeting: A Practical Approach, 1st ed. IRL Press, Oxford, pp. 33–62.
Xi, R., Doan, C., Liu, D., Xie, T., 2005. Pelota controls self-renewal of germline stem cells by repressing a Bam-independent differentiation pathway. Development 132, 5365–5374.
Xu, X., Pantakani, D.V., Luhrig, S., Tan, X., Khromov, T., Nolte, J., Dressel, R., Zechner, U., Engel, W., 2011. Stage-specific germ-cell marker genes are expressed in all mouse pluripotent cell types and emerge early during induced pluripotency. PLoS One 6, e22413.
Yadav, P.S., Prashar, P., Bandyopadhyay, A., 2012. BRITER: a BMP responsive osteoblast reporter cell line. PLoS One 7, e37134.
Yamamoto, M., Saijoh, Y., Perea-Gomez, A., Shawlot, W., Behringer, R.R., Ang, S.L., Hamada, H., Meno, C., 2004. Nodal antagonists regulate formation of the anteroposterior axis of the mouse embryo. Nature 428, 387–392.

Yang, D.H., Smith, E.R., Roland, I.H., Sheng, Z., He, J., Martin, W.D., Hamilton, T.C., Lambeth, J.D., Xu, X.X., 2002. Disabled-2 is essential for endodermal cell positioning and structure formation during mouse embryogenesis. Dev. Biol. 251, 27–44.

Zimmerman, L.B., De Jesús-Escobar, J.M., Harland, R.M., 1996. The Spemann organizer signal noggin binds and inactivates bone morphogenetic protein 4. Cell 86, 599–606.